

Supplementary material

In-Depth Characterization of Choline Lysinate ([Cho][Lys]) in Ethylene Glycol for Optimized CO₂ Capture Conditions

Silvia Mazzotta^{1,2,4*}, Giuseppe Ferraro^{3*}, Anna Vittoria De Napoli^{1,3}, Stefania Lettieri³, Francesca Cardano⁵, Francesca Verga^{1,2}, Candido F. Pirri^{1,3}, and Sergio Bocchini^{1,3}

¹ Center for Sustainable Future Technologies Istituto Italiano di Tecnologia. Via Livorno 60, Torino 10144, Italy

² Dipartimento di Ingegneria dell'Ambiente, del Territorio e delle Infrastrutture (DIATI) Politecnico di Torino. Corso Duca degli Abruzzi 24, Torino 10129, Italy

³ Dipartimento di Scienza Applicata e Tecnologia (DISAT), Politecnico di Torino. Corso Duca degli Abruzzi 24, Torino 10129, Italy

⁴ Scuola Universitaria Superiore (IUSS) Pavia. Palazzo del Broletto-Piazza della Vittoria 15, Pavia 27100, Italy

⁵ Dipartimento di Chimica, Università di Torino. Via Pietro Giuria 7, Torino 10125, Italy

* Corresponding author: giuseppe.ferraro@polito.it, silvia.mazzotta@iusspavia.it

ATR

The ionic liquids were initially characterized as-is through ATR-IR spectroscopy, aiming to demonstrate successful synthesis and, identify the major spectral bands of the amino acid fractions directly involved in the CO₂ absorption process. The ATR-IR spectra of [Cho][Lys] (all collected immediately after solvent removal in the rotary evaporator) are depicted in Figure S1, and S2 respectively, in the spectral region spanning from 4000 to 500 cm⁻¹.

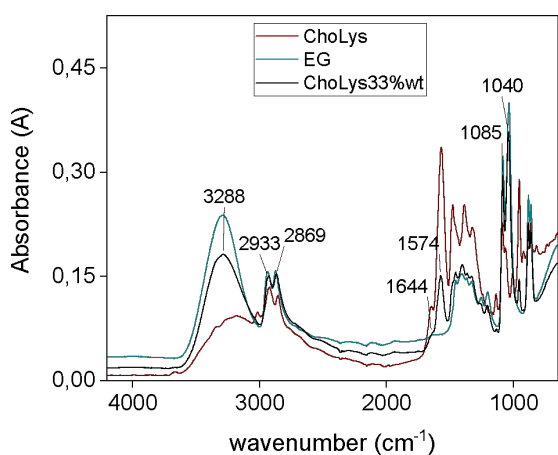


Figure S1. Comparison of ATR-IR spectra of [Cho][Lys] (red), [Cho][Lys] 33% wt solution in ethylene glycol (black), and ethylene glycol (blue).

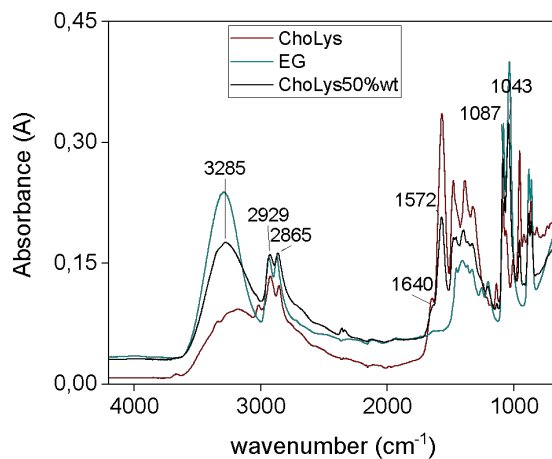
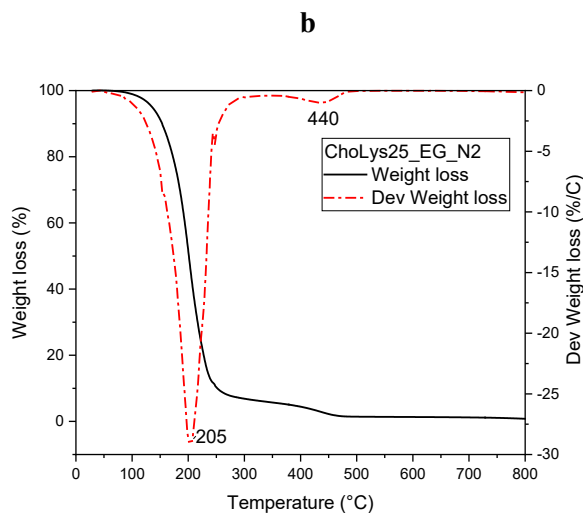
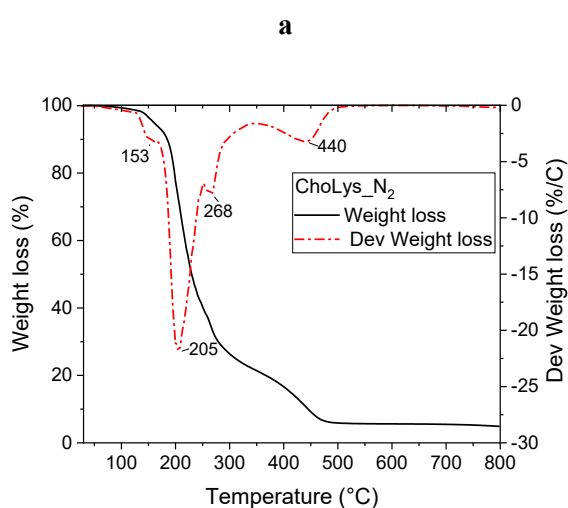


Figure S2. Comparison of ATR-IR spectra of [Cho][Lys] (black), [Cho][Lys] 50% wt solution in ethylene glycol (red), and ethylene glycol (blue).

TGA-IR Analysis

Figure S3. All thermograms were conducted from 25°C to 800°C at a heating rate of 20°C/min, under a 50 ml/min N₂ flux.

- Thermogram of pure [Cho][Lys];
- Thermogram of [Cho][Lys] solution at 25% by weight in Ethylene Glycol;
- Thermogram of [Cho][Lys] solution at 33% by weight in Ethylene Glycol;
- Thermogram of [Cho][Lys] solution at 50% by weight in Ethylene Glycol.



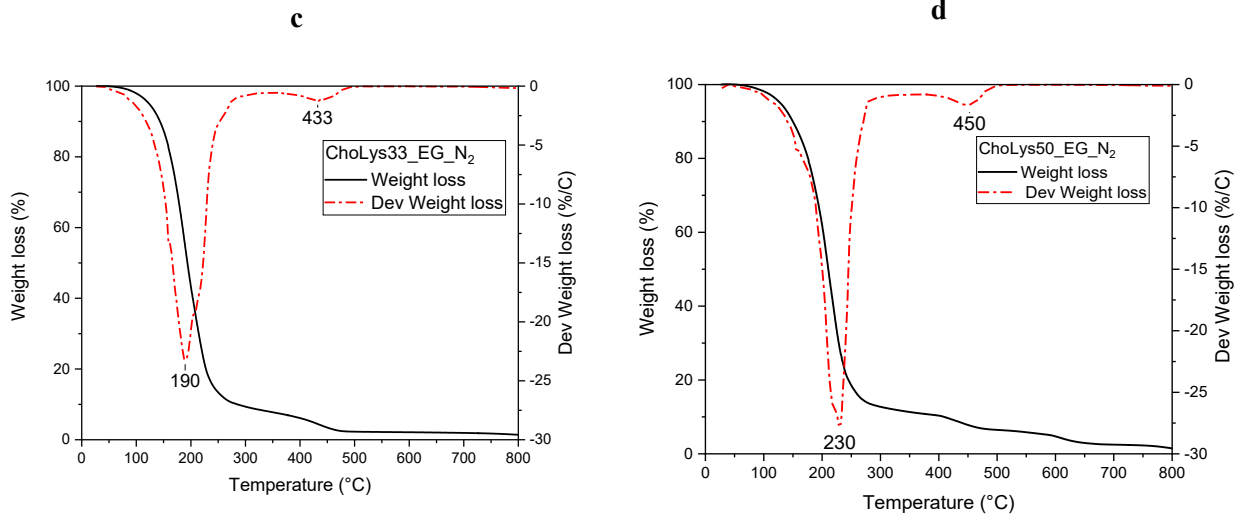


Figure S4. All thermograms were conducted from 25°C to 800°C at a heating rate of 20°C/min, under a combined flux of 30 ml/min Air and 20 ml/min N₂. a) Thermogram of pure [Cho][Lys]; b) Thermogram of [Cho][Lys] solution at 25% by weight in Ethylene Glycol; c) Thermogram of [Cho][Lys] solution at 33% by weight in Ethylene Glycol; d) Thermogram of [Cho][Lys] solution at 50% by weight in Ethylene Glycol.

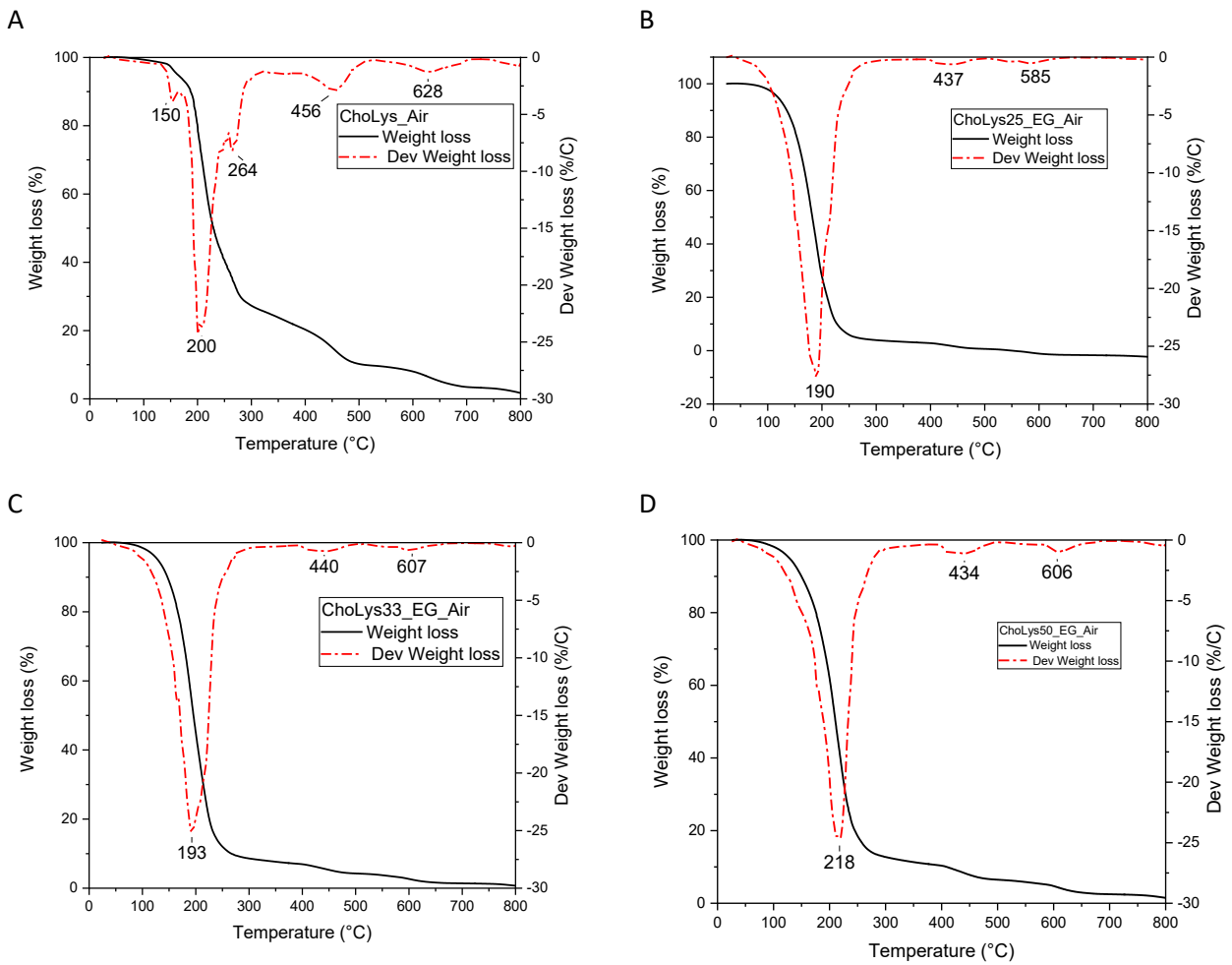


Figure S5. TGA-IR analysis: gas-phase IR spectra of [Cho][Lys] from thermal degradation.

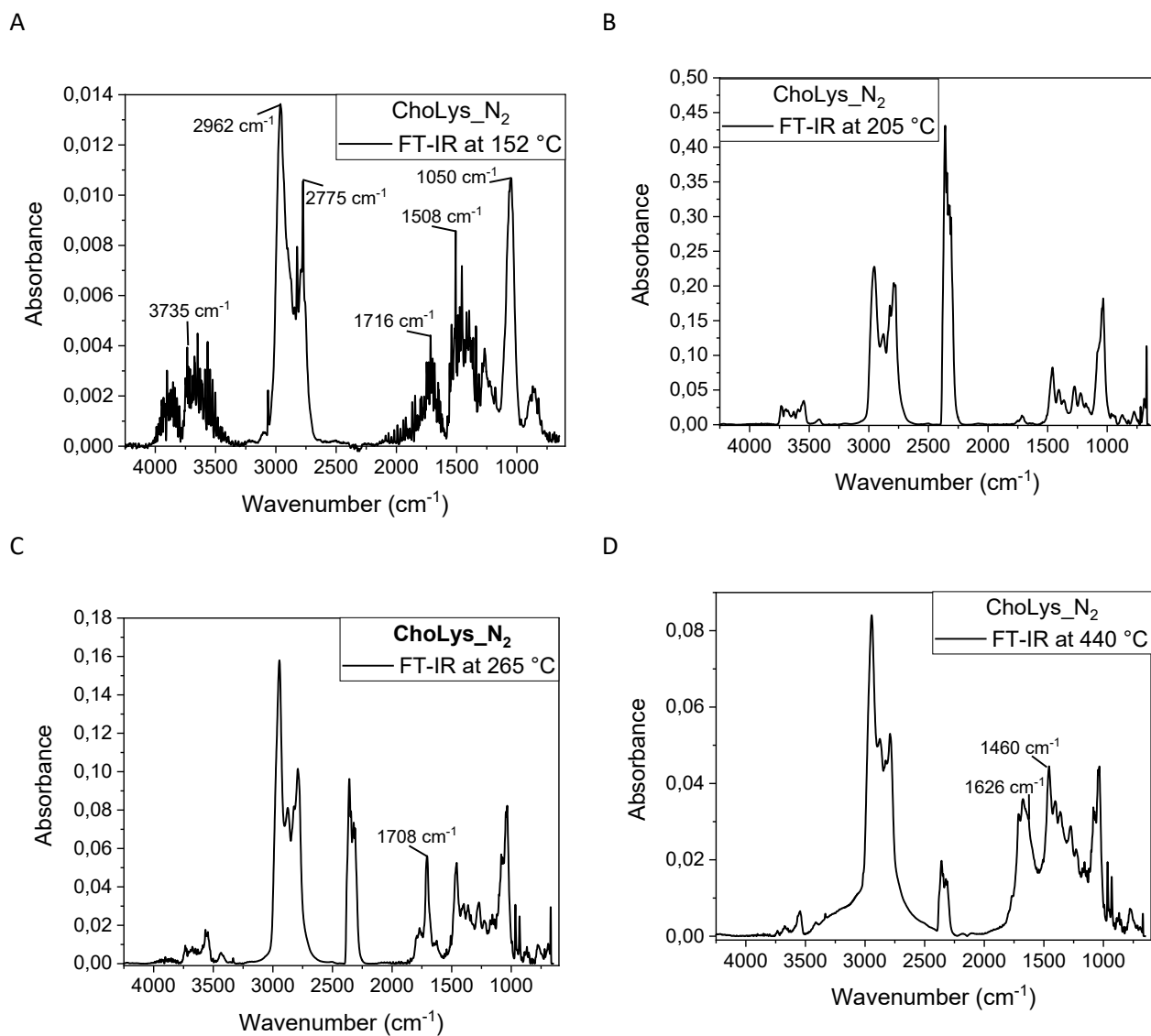
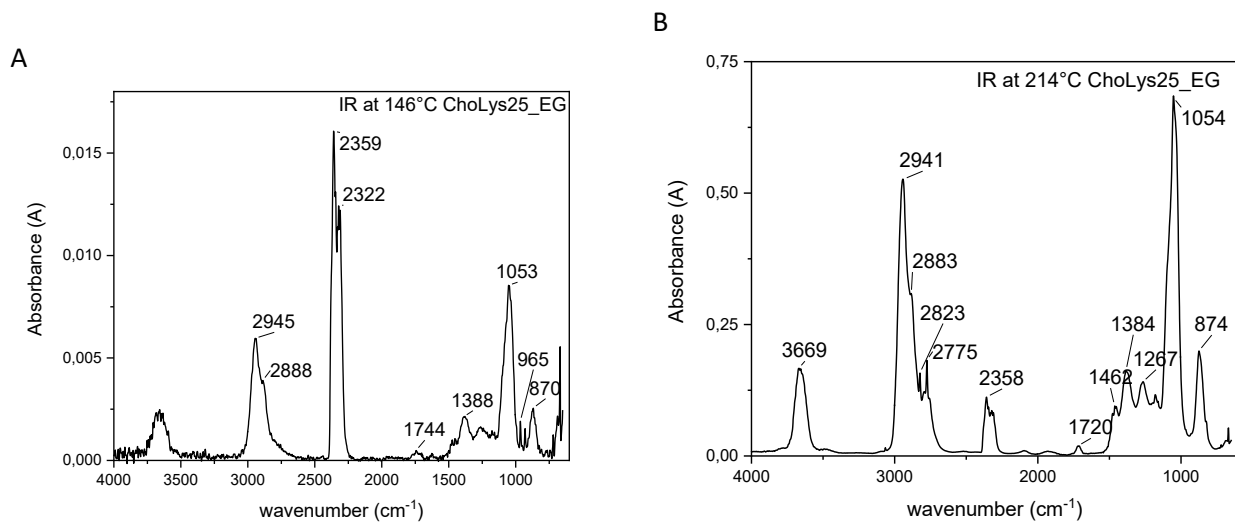


Figure S6. TGA-IR analysis: gas-phase IR spectra of [Cho][Lys]25_EG from thermal degradation.



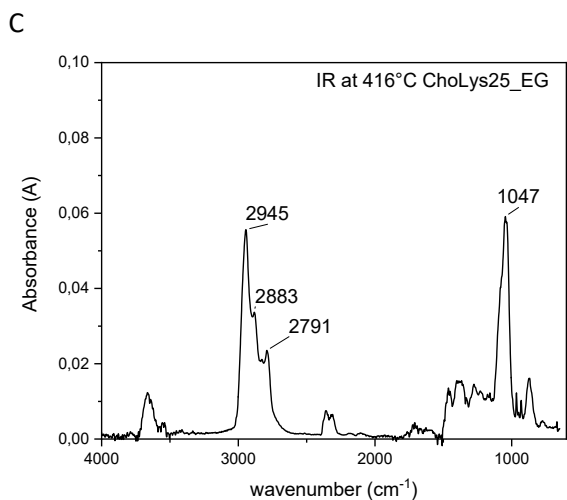


Figure S7. TGA-IR analysis: gas-phase IR spectra of [Cho][Lys]33_EG from thermal degradation.

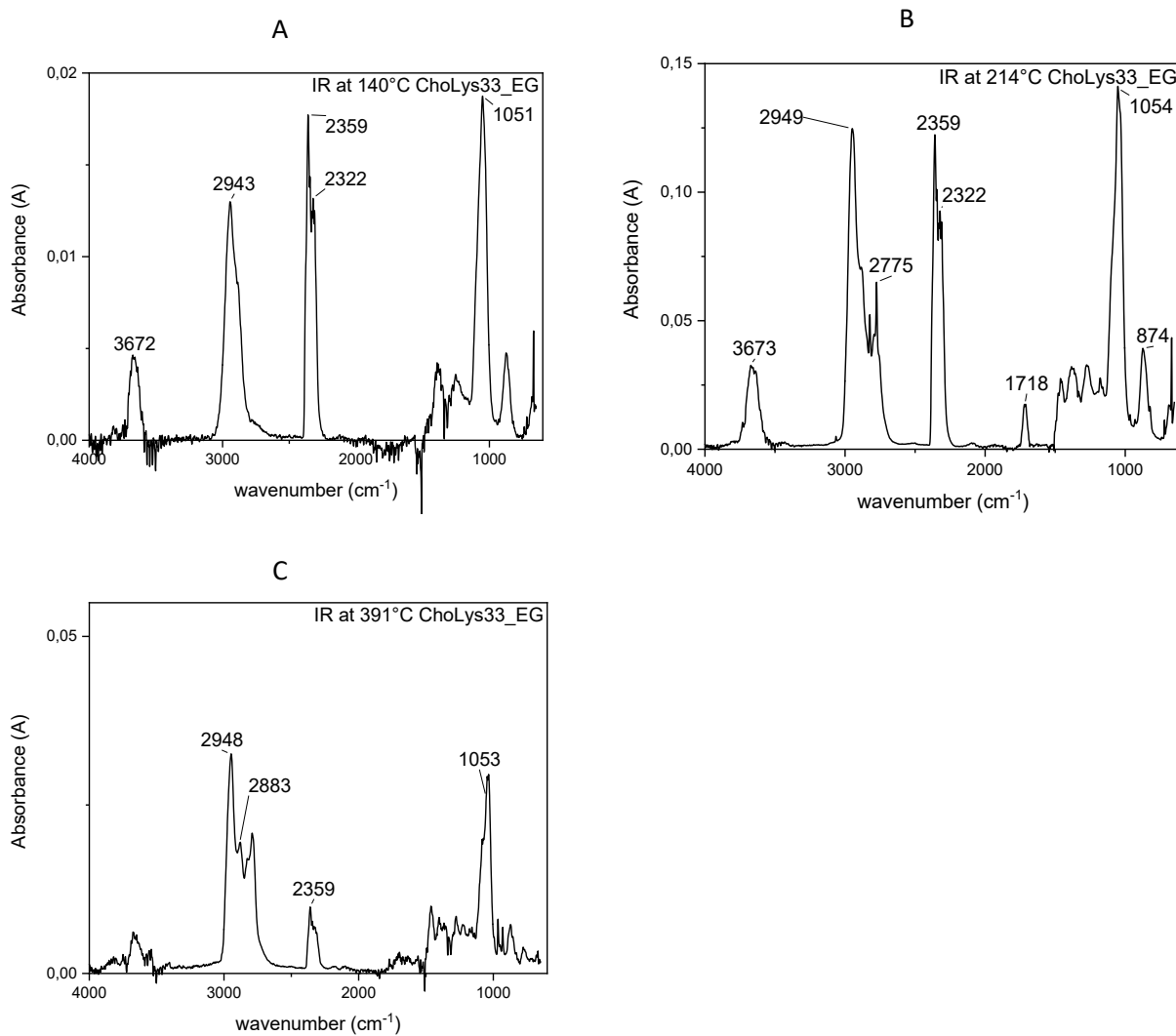
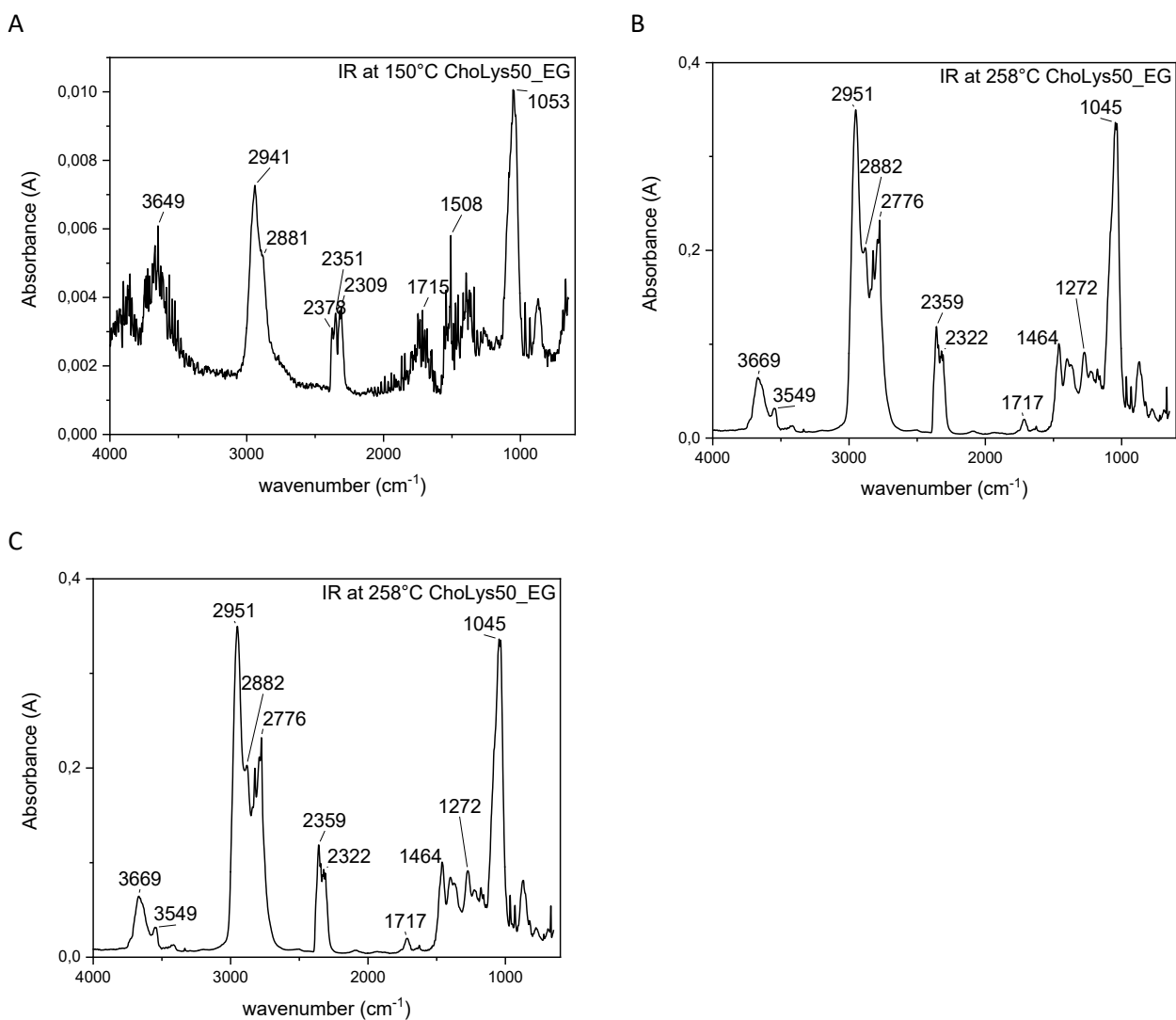
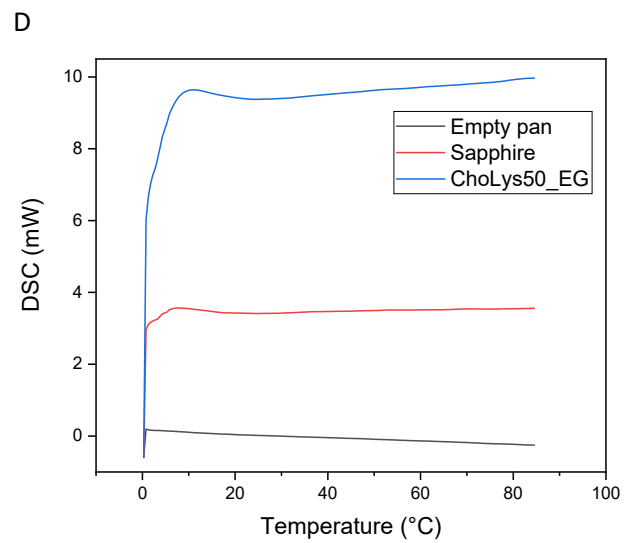
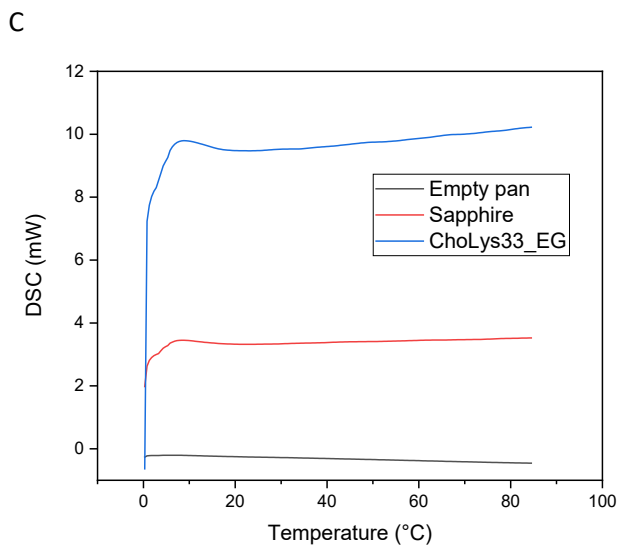
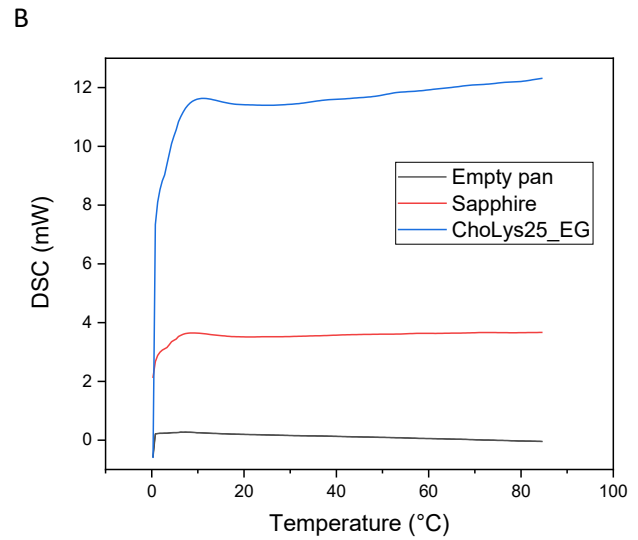
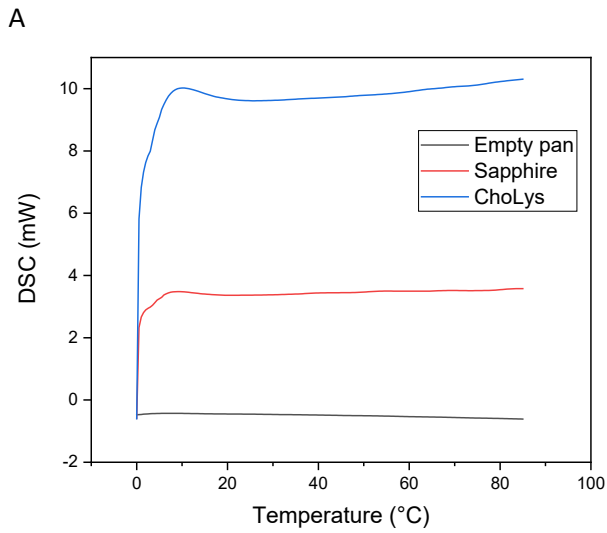


Figure S8. TGA-IR analysis: gas-phase IR spectra of [Cho][Lys]50_EG from thermal degradation.



Heat capacity Cp

Figure S9. Comparison of thermograms for an empty pan, a pan with the reference material (sapphire), and a pan containing the ionic liquid or the ionic liquid solution. Three measurements were conducted under the same conditions, with a temperature range from 0 to +90 °C, at heating rates of 10 °C min⁻¹, under an N₂ flow of 70 ml min⁻¹.



Viscosity

By using a calibrated glass capillary viscometer, such as the Cannon-Fenske viscometer, it is possible to determine the kinematic viscosity, ν , of both transparent and opaque liquids by measuring the time it takes for

the liquid to flow under the influence of gravity. The dynamic viscosity, η , can be obtained by multiplying the kinematic viscosity, ν , by the density, ρ , of the liquid:

$$[6] \quad \eta(\text{cP}) = \nu(\text{cSt}) * \rho(\text{g/cm}^3)$$

The appropriate Cannon-Fenske viscometer should be selected based on the expected viscosity, as each viscometer has a specific measurement range. The viscometer is filled through section I until bubble is reached, and then it is placed in a precision temperature-controlled bath for capillary viscometers (THERMOCAP PLUS, FUNGILAB S.A.). The bath is filled with deionized water and set to the desired temperature. Once the sample is thermostatted, the time it takes for the liquid to flow from point C to point E can be measured. Kinematic viscosity (ν) measurements were taken at 40°C, 50°C, 60°C, and 70°C.

Post-absorption ATR analysis

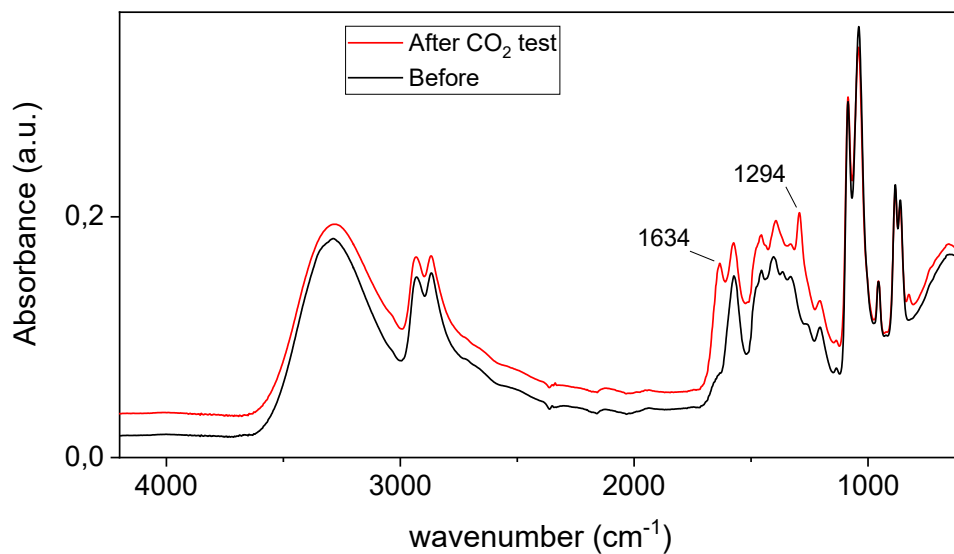


Figure S10. Comparison of ATR-IR spectra of [Cho][Lys] 33% wt in ethylene glycol, before and after the gravimetric absorption test, performed by exposing the ionic liquid solution to a 30 ml/min CO₂ flow.

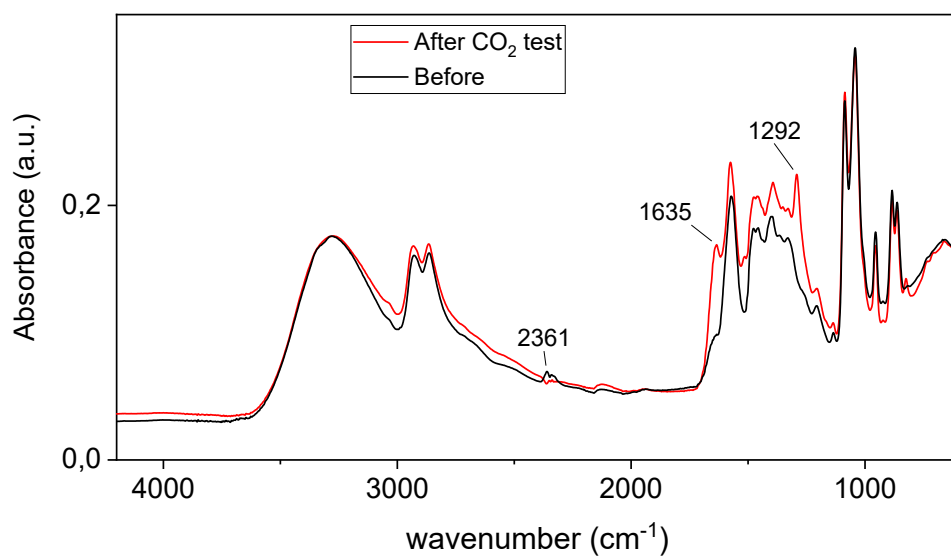


Figure S11. Comparison of ATR-IR spectra of [Cho][Lys] 50% wt in ethylene glycol, before and after the gravimetric absorption test, performed by exposing the ionic liquid solution to a 30 ml/min CO₂ flow.

Post-absorption TGA

Table S1. TGA Analysis under 50 ml/min N2 flux of ionic liquids solutions in ethylene glycol

[Cho][Lys] (%wt)	T On set (°C)	Temperature of maximum degradation rate
25	152.2	192
33	159.9	202.8
50	140.5	213.4

Figure S12. Thermograms of [Cho][Lys] solutions at 25 wt% in Ethylene Glycol

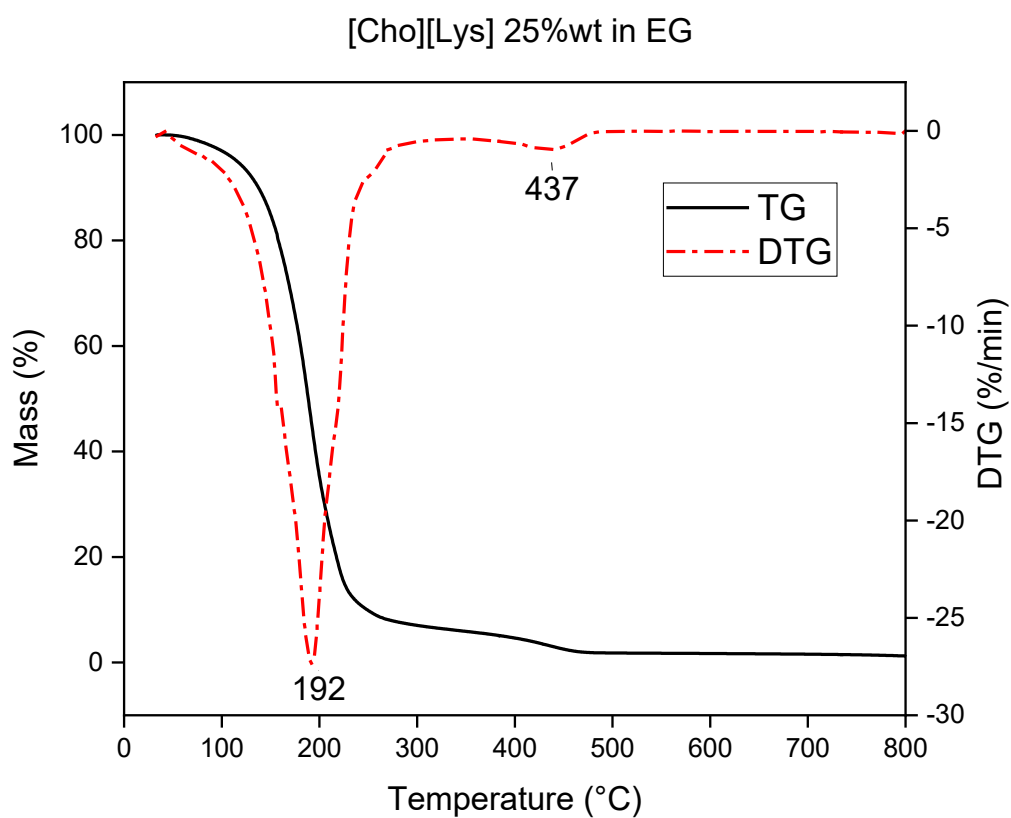
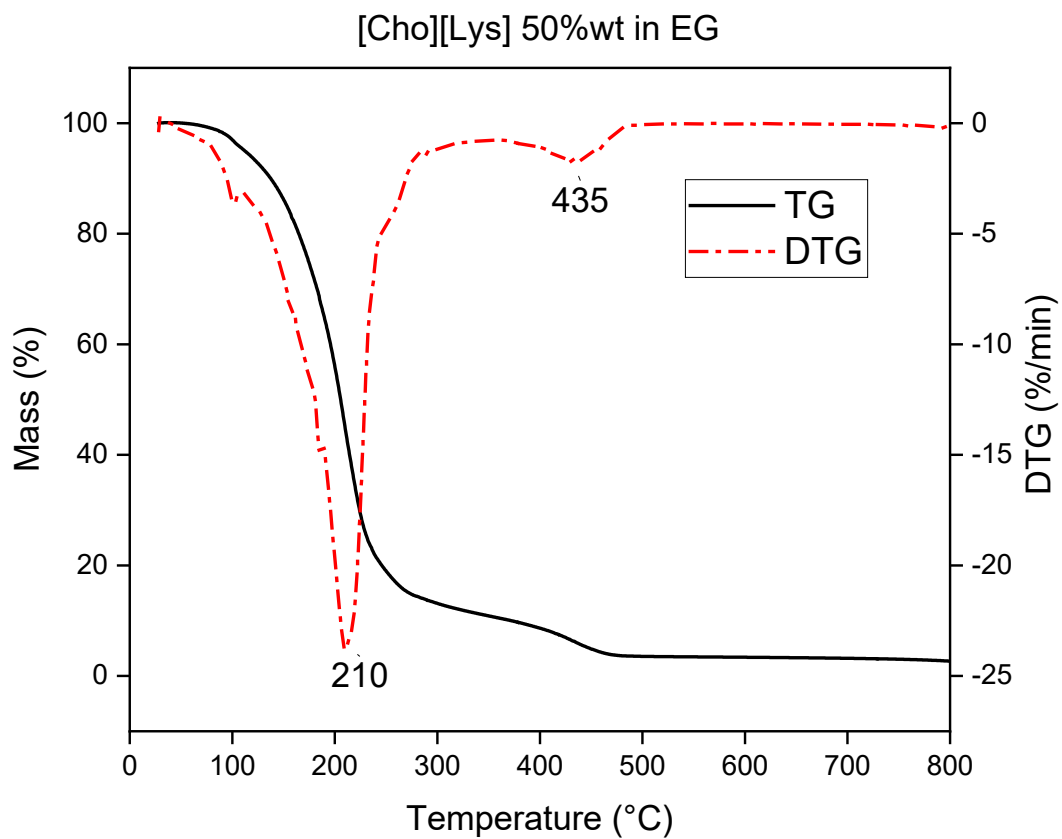


Figure S13. Thermograms of [Cho][Lys] solutions at 50 wt% in Ethylene Glycol

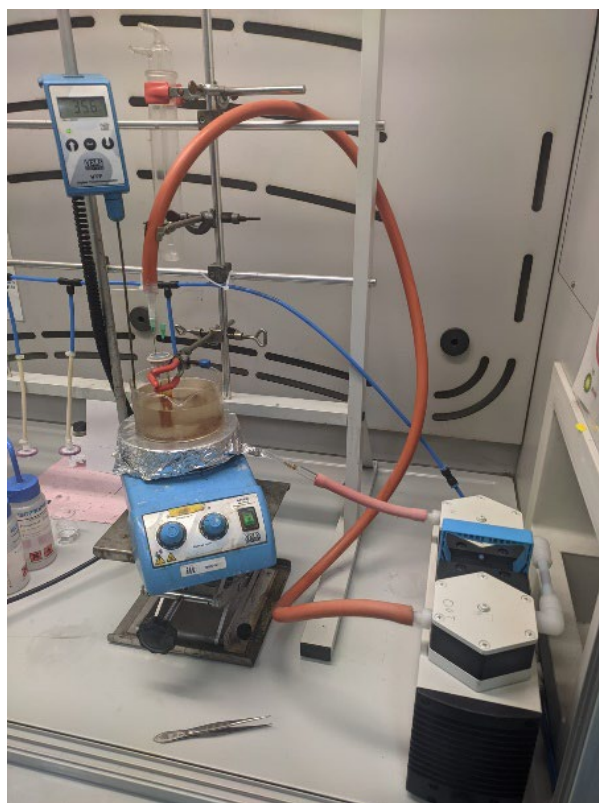


Aging process

The aging process was carried out by heating the ionic liquid to 80 °C by means of a silicone oil bath on a magnetic plate that ensured proper mixing by a stirring rod.

At the same time by needle and pump, air was constantly insufflated directly inside the ionic liquid during the entire process with a total duration of 168 hours (one week).

Figure S14. Aging process set-up of [Cho][Lys]33_EG



Absorbance Trend Estimation

Experimental Values of Carbon Capture test under 100% CO₂ flux

The weights are plotted as a function of time and then interpolated using Origin pro 2018 software. A type 1 decay exponential function was used whereby the $l' y_0$ gives the plateau value achieved for each solution while $k=1/t_1$ is the decay rate i.e., a parameter indicating how quickly each sample absorbs CO₂.

Table S2 - [Cho][Lys] 25% EG

Points	Time (min)	Weight (g)
1	15	28.08354
2	30	28.10403
3	45	28.11183
4	60	28.11777
5	75	28.12018
6	90	28.1212

7	105	28.12164
8	120	28.12156

Figure S7. Graphical representation of carbon capture test results for [Cho][Lys] 25% in EG.

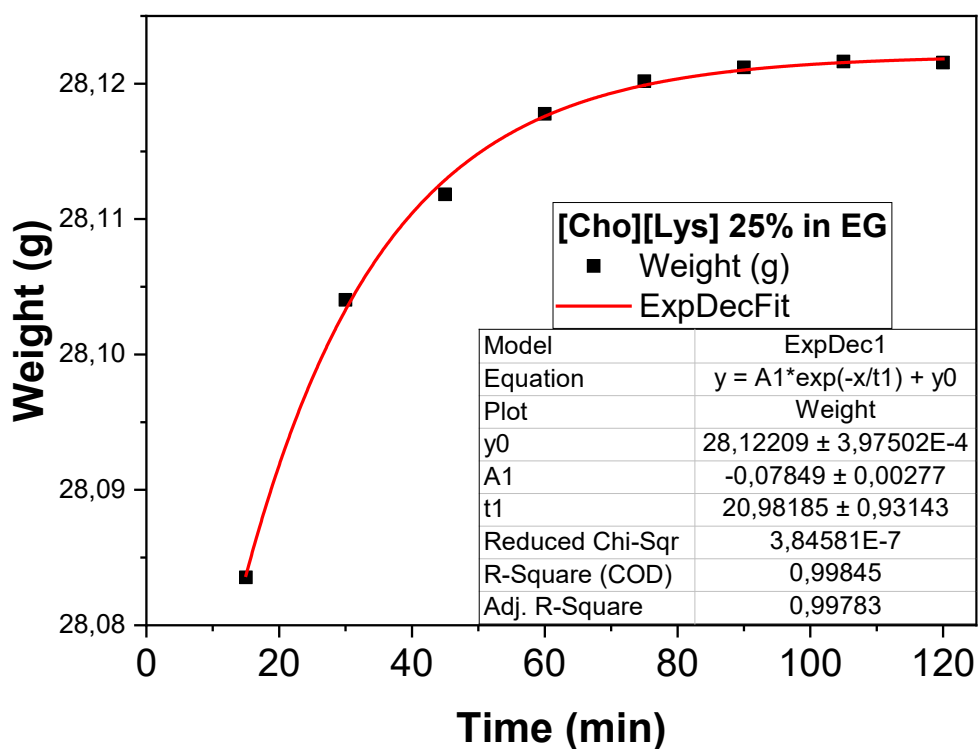


Table S3 - [Cho][Lys] 33% EG

Points	Time (min)	Weight (g)
1	15	28.24586
2	30	28.2639
3	45	28.27753
4	60	28.28668
5	75	28.29266
6	90	28.29652

7	105	28.29796
8	120	28.29923
9	135	28.29969
10	150	28.29997
11	165	28.29989
12	215	28.29955
13	265	28.29930

Figure S8. Graphical representation of carbon capture test results for [Cho][Lys] 33% in EG.

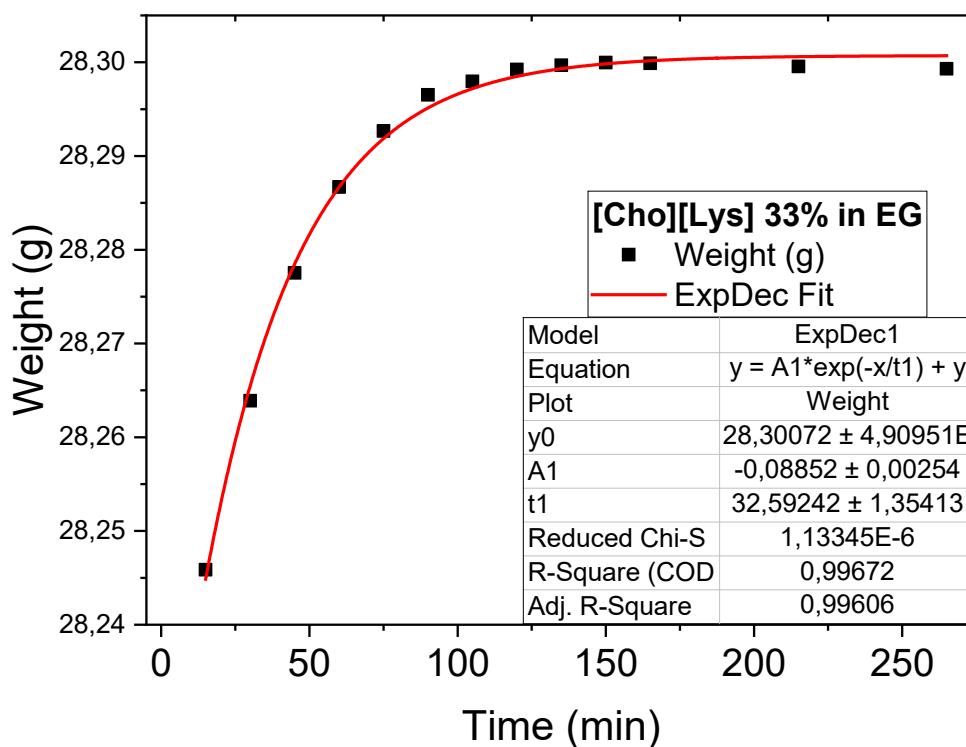


Table S4 - [Cho][Lys] 50% EG

Points	Time (min)	Weight (g)
--------	------------	------------

1	15	27.77048
2	30	27.78599
3	45	27.80735
4	60	27.82423
5	75	27.82816
6	90	27.83091
7	105	27.83109
8	120	27.83096

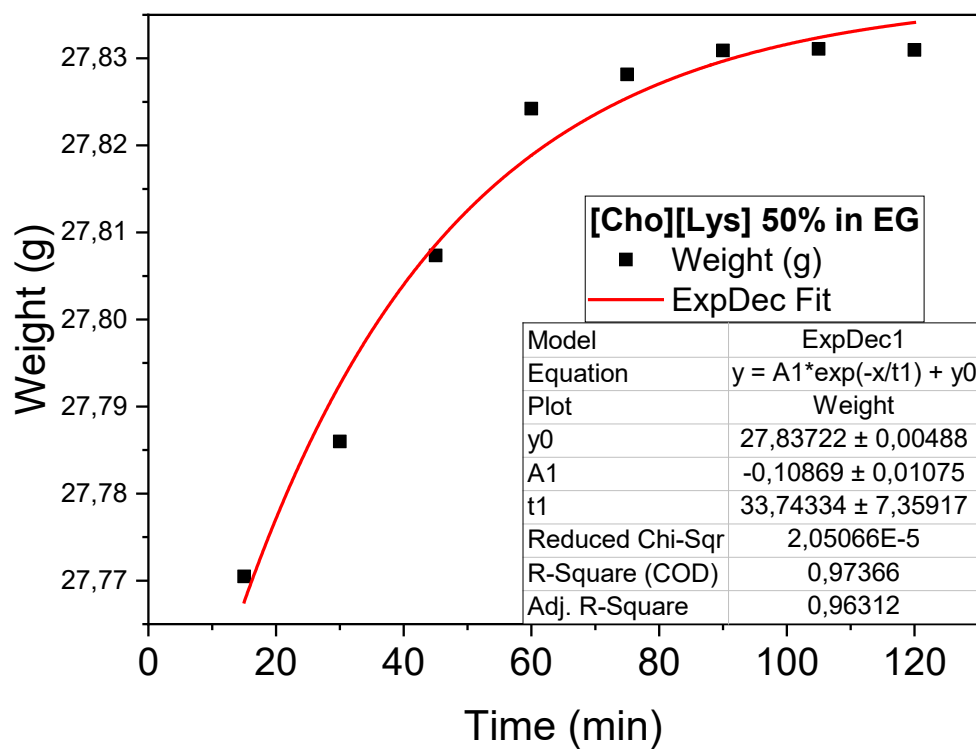


Table S5 – comparison of [Cho][Lys] solution in EG decay rate

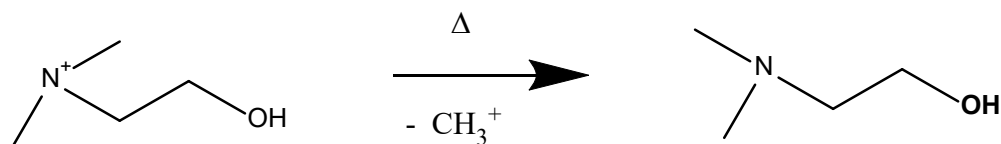
[Cho][Lys] (%wt)	t1	k=1/t1
25	20.98185	0.04766

33	32.59242	0.00127
----	----------	---------

50	33.74334	0.02964
----	----------	---------

Proposed degradation pathway of the choline moiety:

Upon thermal stress, the choline cation ($[\text{HO-CH}_2\text{-CH}_2\text{-N}^+(\text{CH}_3)_3]$) is known to undergo Hofmann-type elimination or fragmentation reactions. A plausible route involves the loss of a methyl group as CH_3^+ or its equivalent, followed by the rearrangement of the remaining structure to yield dimethylaminoethanol (DMAE):



This mechanism is consistent with literature reports on the thermal degradation of quaternary ammonium compounds and is supported by our TGA-IR data. The spectral fingerprint of the evolved gas phase matches perfectly with the roto-vibrational features of DMAE in the gas phase, as seen in Figure S5, where a direct comparison with the reference spectrum is provided.

Multi-cycle CO₂ Absorption Test

To evaluate the reproducibility and regeneration capability of the IL solution, multi-cycle CO₂ absorption tests were performed. The [Cho][Lys] 25 wt% solution in ethylene glycol was placed in a custom glass reactor (4.5 mL total volume, 3 mL of liquid), thermostated at 30 °C and stirred at 500 rpm. CO₂ gas (99.9%) was bubbled through the solution at a flow rate of 50 mL/min.

Absorption cycles were monitored by recording the outlet CO₂ concentration as a function of time via an inline infrared detector. Each cycle lasted until saturation was reached. Desorption was carried out by heating the solution under N₂ (50 mL/min) at 65 °C for 30 minutes.

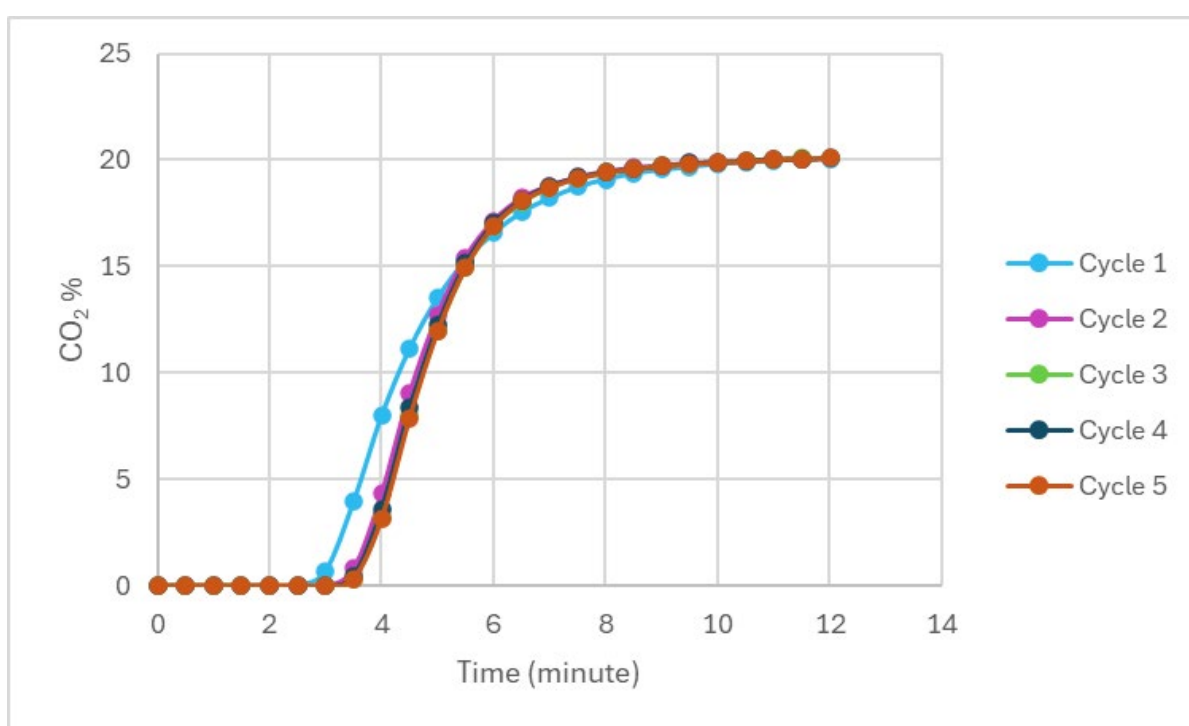


Figure S15. CO₂ absorption profiles over multiple cycles for [Cho][Lys] 25% wt in ethylene glycol.

CO₂ concentration at the outlet of the reactor was normalized to its initial value and plotted as a function of time. The data were collected during repeated absorption-desorption experiments under constant CO₂ flow (50 mL/min) at 30 °C. Between each cycle, the solution was regenerated by mild heating under N₂ atmosphere. As observed, absorption in the second cycle is noticeably faster and more efficient than in the first, as demonstrated by the steeper decline and lower plateau. This qualitative improvement supports the hypothesis of kinetic activation or rearrangement of the ionic environment following the first exposure to CO₂.

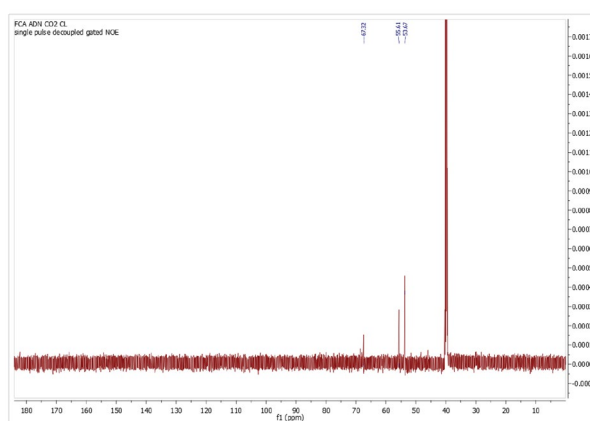
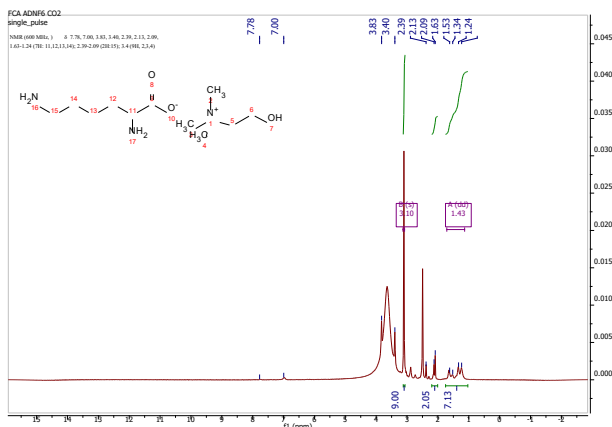
NMR

The NMR spectra were recorded on a JEOL ECZ-R 600 MHz, spectrometer at 25 °C using DMSO-d₆. Spectra were reported as chemical shifts (δ) in ppm relative to DMSO-d₆ signal as reference and processed by MNova software.

The water signal observed in the ¹H NMR spectrum arises from the trace moisture typically present in the deuterated solvent. Unfortunately, this overlaps with the characteristic signals corresponding to the four protons of the two CH₂ groups in choline chloride, preventing quantitative determination of water content [REF for choline chloride NMR: https://www.chemicalbook.com/SpectrumEN_67-48-1_1HNMR.htm].

The signals corresponding to the three methyl groups are clearly visible around 3 ppm. Regarding the lysinate, the methylene protons within the aliphatic chain and the α -proton appear in the 1.5–2 ppm range, while the signal at approximately 2.09 ppm is attributed to the two protons of the CH₂ group adjacent to the terminal amine. Around 7.00 and 7.78 ppm, two broad peaks are observed, corresponding to the amine protons. However, as reported in the literature, these protons undergo rapid exchange, making quantitative analysis unfeasible.

[https://www.google.com/search?sca_esv=4e4b5f70bf6a4414&rlz=1C1VDKB_itIT1110IT1110&sxsr=A3TifNJqSS5Ug-Q3p52oIxy1Z0U-tqUVw:1754380111990&q=lysinate++nmr+spectrum+dmsod6&source=Inms&fbs=AlljpHyQhmcRdwysNp0H4fUJo6s5eOtNb8ZNcymYPhjpCSkbN7z_5B0ZKtpqIIf9xC-NbYvXcYuxVW9aaJrbkwW4BicF_9SjQ1mG0G5rCyVH97GTv-QOS7tMZQV_0HAvSotDhIzMxS-8vvs0Ew8rkfK_8TQ7tVrc6Jwwifqw4C9zah5J16LX0eoqmdBfEacjYEAUUY0zcMSPZiYZNx4vKcUuLg9D Wx6g&sa=X&ved=2ahUKEwjnhIGbl_OOaxX58rsIHf0qAZwQ0pQJegQIDhAB&biw=1440&bih=791&dpf=2]



Unfortunately, under the experimental conditions used in this study, recording meaningful ¹³C NMR data is not feasible. The high concentration of non-deuterated solvent in our working formulations produces intense

solvent signals and broad background noise, which mask weaker resonances. At the concentrations relevant for our CO₂ absorption tests, this results in an insufficient signal-to-noise ratio for detecting the expected carbamate/carbonyl resonances in the 160–170 ppm range.

Even after prolonged acquisition times, the anticipated carbonyl and carbamate peaks remained too weak to be confidently assigned, while only the more intense choline carbon signals (54, 55, and 67 ppm, [REF: https://www.chemicalbook.com/SpectrumEN_67-48-1_13CNMR.htm]) and lysine backbone carbons could be observed. Signals from the ϵ -CH₂ group overlapped with those of DMSO-d₆, further complicating analysis.

(Claridge, *High-Resolution NMR Techniques in Organic Chemistry*, 3rd ed., Elsevier, 2016).